

Bayesian learning of Causal Structure and Mechanisms with GFlowNets and Variational Bayes

Mizu Nishikawa-Toomey*
Mila, Université de Montréal

MIZU.NISHIKAWA-TOOMEY@MILA.QUEBEC

Tristan Deleu*
Mila, Université de Montréal

DELEUTRI@MILA.QUEBEC

Jithendaraa Subramanian
Mila, McGill

JITHENDARAA.SUBRAMANIAN@MILA.QUEBEC

Yoshua Bengio
Mila, Université de Montréal

YOSHUA.BENGIO@MILA.QUEBEC

Laurent Charlin
Mila, HEC Montréal

LCHARLIN@MILA.QUEBEC

Abstract

Bayesian causal structure learning aims to learn a posterior distribution over directed acyclic graphs (DAGs), and the mechanisms that define the relationship between parent and child variables. By taking a Bayesian approach, it is possible to reason about the uncertainty of the causal model. The notion of modelling the uncertainty over models is particularly crucial for causal structure learning since the model could be unidentifiable when given only a finite amount of observational data. In this paper, we introduce a novel method to jointly learn the structure and mechanisms of the causal model using Variational Bayes, which we call Variational Bayes-DAG-GFlowNet (VBG). We extend the method of Bayesian causal structure learning using GFlowNets to learn not only the posterior distribution over the structure, but also the parameters of a linear-Gaussian model. Our results on simulated data suggest that VBG is competitive against several baselines in modelling the posterior over DAGs and mechanisms, while offering several advantages over existing methods, including the guarantee to sample acyclic graphs, and the flexibility to generalize to non-linear causal mechanisms.

Keywords: Bayesian modelling, Bayesian causal structure learning, causality, Bayesian networks, uncertainty estimation

1. Introduction

Bayesian networks (Pearl, 1988) represent the relationships between random variables as Directed Acyclic Graphs (DAGs). This modelling choice allows for inspecting of the conditional independence relations between random variables in a visual and straightforward manner. A Bayesian network can be used to represent a joint distribution over its variables. A *causal* Bayesian network, or a causal model, defines a family of distributions with shared parameters, corresponding to all possible interventions on the variables (Peters et al., 2017). Causal models allow for questions of importance to be answered such as: can we find an intervention that will result in the desired outcome in the modelled system? Answering these questions using causal models has been prominent

* Equal contributions

in fields such as genetics (Belyaeva et al., 2021), medical diagnosis (Chowdhury et al., 2020) and economics (Awokuse, 2005).

In the last few decades, many algorithms have been suggested for learning a causal model compatible with the data. The challenge of causal modelling lies in the fact that the search space of all possible DAGs grows super-exponentially in the number of nodes. As a result, many different heuristic methods have been suggested to tackle this problem. In addition to finding the graph, quantifying the uncertainty over causal models poses another challenge. Since observational data alone only identifies the Markov equivalence class of DAGs (Verma and Pearl, 1990), graph-finding algorithms that capture the uncertainty of the whole Markov equivalence class are beneficial, e.g., to avoid confidently wrong predictions or to explore in a way that will minimize this uncertainty. Reducing this uncertainty about the causal model requires interventions in the real world (Pearl, 2000) that could be prohibitively expensive, and quantifying uncertainty to direct the most informative interventions is a topic of particular interest in causal modelling.

Recently, a host of Bayesian causal structure learning algorithms that leverage the recent advances in gradient descent methods have been proposed (Lorch et al., 2021; Cundy et al., 2021; Deleu et al., 2022; Annadani et al., 2021). Each of these methods infers different aspects of the causal model and its uncertainty, given some assumptions on the model. The DAG-GFlowNet algorithm (Deleu et al., 2022) promises a unique way of modelling a distribution over DAGs using GFlowNets (Bengio et al., 2021a,b). However, until this point, it has been limited to inferring only the DAG structure, without explicitly inferring the parameters of the causal mechanisms.

In this paper, we introduce an extension of DAG-GFlowNet which we call *Variational Bayes DAG-GFlowNet* (VBG), which infers the parameters of a linear Gaussian model between continuous random variables in the DAG, along with the graph itself, using Variational Bayes. This lends itself well to active learning approaches in causal modelling which are of great interest (Scherrer et al., 2021; Agrawal et al., 2019; Tigas et al., 2022; Toth et al., 2022), since conducting interventions to gather data for causal modelling is often very resource heavy. We address the pitfalls of other Bayesian causal structure learning algorithms that model the mechanisms and the graphs. DiBS (Lorch et al., 2021) lacks the ability to sample from the posterior in an unbounded manner once the model is trained, and acyclicity is not guaranteed throughout training iterations, similarly, VCN (Annadani et al., 2021) does not guarantee acyclicity, BCD Nets (Cundy et al., 2021) does not allow for flexibility of model parametrization for the mechanisms. Our method overcomes all these pitfalls and does comparatively well to these methods in our empirical evaluation using a number of metrics. In addition, we believe that this novel approach of finding the causal model using Variational Bayes has the potential to be applied to other Bayesian causal structure learning algorithms that only model the graph, and expand their capabilities to also model the mechanisms.

2. Related work

2.1. Causal structure learning

This paper contributes to the large body of work on causal structure learning, and relates most closely to *score-based methods* for causal discovery (Chickering, 2003; Tsamardinos et al., 2006). Score-based methods consist of two parts: defining a score which determines how well a DAG fits the observed data, and a search algorithm to search over the space of possible DAGs, to return the DAG with the highest score. Examples of scores include the Bayesian Gaussian equivalent (BGe) score (Geiger and Heckerman, 2013) for linear-Gaussian models, and the Bayesian Dirich-

let equivalent (BDe) score (Chickering et al., 1995) for Dirichlet-multinomial models. The BGe score and the BDe score represent different ways to compute the marginal likelihood $P(\mathcal{D} | G)$, depending on the assumptions of the model: by using conjugate priors and likelihoods, the mechanisms parameters can be marginalised out in closed form. A subclass of score-based methods provides the exact identification of causal models from observational data using parametric assumptions (Hoyer et al., 2008; Shimizu et al., 2006). The modelling assumptions of (Shimizu et al., 2006) show that if the mechanisms are linear and the noise is non-Gaussian, observational data is sufficient to identify the graph.

One of the more recent algorithms that resulted in a series of papers demonstrating its applications is the NO-TEARS framework (Zheng et al., 2018). In NO-TEARS, the score-based approach searching across discrete space with a hard constraint is relaxed into a soft constraint by using a differentiable function $h(W)$, which expresses the ‘‘DAG-ness’’ of a weighted adjacency graph W . This led to the development of new causal structure learning algorithms using observational and interventional data, even with non-linear causal mechanisms (Lachapelle et al., 2019; Ke et al., 2019; Brouillard et al., 2020).

2.2. Bayesian causal structure learning

Bayesian approaches to structure learning involve learning a distribution over the graph and parameters of the mechanisms of causal models. However, computing the exact posterior from data requires calculating the evidence, $p(\mathcal{D}) = \sum_G \int_{\theta} P(\mathcal{D} | G, \theta) P(G, \theta) d\theta$. This becomes quickly intractable as it involves enumerating over graphs and all possible parameters. As a result, variational inference or MCMC techniques are often used to obtain an approximate posterior over the graph and parameters. DiBS (Lorch et al., 2021) employs variational inference over a latent variable that conditions the graph distribution to approximate the posterior, in addition to the constraint proposed in (Zheng et al., 2018) as a soft prior, to perform marginal or joint Bayesian structure learning in nonlinear or linear Gaussian models. VCN (Annadani et al., 2021) is in a similar setup, but infers only the structure and attempts to capture a multimodal posterior by autoregressively predicting edges in the graph. However, due to the soft DAG-ness prior in both these methods, samples from the posterior approximation are not guaranteed to be valid DAGs. Similarly, Ke et al. (2022) define a distribution over graphs in an autoregressive way, but do not enforce acyclicity. BCD Nets (Cundy et al., 2021) parametrize a distribution over DAGs as a distribution over upper-triangular weighted and permutation matrices, that once combined together induces a distribution over weighted adjacency matrices. This method is guaranteed to output only DAGs without the need for the soft DAG-ness constraint; however, it is only limited to linear-Gaussian models. Wang et al. (2022) uses sum-product networks that define a topological ordering and then use variational inference to learn an approximate posterior. The structure MCMC algorithm (Madigan and York, 1995) build a Markov chain over DAGs by adding or removing edges. One of the motivations for learning a distribution over the causal model is that it lends well to active causal structure learning (Scherrer et al., 2021; Agrawal et al., 2019; Tigas et al., 2022; Toth et al., 2022). By knowing more about what the model is uncertain about, it becomes possible to choose the interventions that will result in the maximum reduction in the uncertainty of the causal model.

3. Background

3.1. Causal modelling

We study causal models described by a triple (G, f, σ^2) , where G is the causal graph, f represents the mechanisms between child-parent pairs, i.e., how a set of parent nodes influence a child node and σ^2 is the noise associated with each random variable in the graph. Assuming the Markov condition, the likelihood can therefore be factorized according to the following DAG formulation:

$$P(X | G, \theta) = \prod_{n=1}^N \prod_{k=1}^K P(X_k^{(n)} | \text{Pa}_G(X_k^{(n)}), \theta_k), \quad (1)$$

where K is the number of nodes in the graph, N is the number of independent samples from the causal model, and $\text{Pa}_G(X_k)$ are the parents of X_k in the graph G . θ represents the parameters of the cause-effect mechanism, which we will call *mechanism parameters*. If we assume that the model has linear mechanisms with Gaussian noise (often called a linear-Gaussian model), then the mechanism parameters θ correspond to a matrix of *edge weights* θ_{ik} representing the strength of the connection between a parent X_i and a child X_k , through the following functional relation:

$$X_k = \sum_{i=1}^K \mathbb{1}(X_i \in \text{Pa}_G(X_k)) \theta_{ik} X_i + \varepsilon_k \quad \text{with} \quad \varepsilon_k \sim \mathcal{N}(0, \sigma^2). \quad (2)$$

It is well-known in causal modelling that a causal graph can in general only be identified up to its Markov equivalence class (MEC) given just observational data (Verma and Pearl, 1990). By introducing appropriate and enough interventional data, it is possible to narrow down the ambiguity to a single graph within a MEC. Given a dataset of observations \mathcal{D} , our goal in this paper is to model the joint posterior distribution $P(G, \theta | \mathcal{D})$ over graph structures G and mechanism parameters θ .

3.2. Generative Flow Networks

Generative Flow Networks (GFlowNets; Bengio et al., 2021a) are generative models learning a policy capable of modelling a distribution over objects constructed through a sequence of steps. A GFlowNet has a training objective such that when the objective is globally minimized, it samples an object x with probability proportional to a given reward function $R(x)$. The generative policy stochastically makes a sequence of transitions, each of which transforms a state s (in an RL sense) into another s' , with probability $P_F(s' | s)$ starting at a single source state s_0 , and such that the set of all possible states and transitions between them forms a directed acyclic graph. The sequence of steps to construct an object is called a “trajectory”.

In addition to the structured state space, every transition $s \rightarrow s'$ in a GFlowNet is associated with *flow* functions $F_\phi(s \rightarrow s')$ and $F_\phi(s)$ on edges and states respectively, typically parametrized by neural networks. The GFlowNet is trained in order to satisfy as well as possible the following flow-matching conditions for all states s' :

$$\sum_{s \in \text{Pa}(s')} F_\phi(s \rightarrow s') = \sum_{s'' \in \text{Ch}(s')} F_\phi(s' \rightarrow s'') + R(s'), \quad (3)$$

where $\text{Pa}(s')$ and $\text{Ch}(s')$ are respectively the parents and children of s' , and $R(s')$ is non-zero only at the end of a trajectory, when $s' = x$ is a fully-formed object. Intuitively, the LHS of (3)

corresponds to the total incoming flow into s' , and the RHS corresponds to the total outgoing flow from s' . If these conditions are satisfied for all states s' , then an object x can be sampled with probability $\propto R(x)$ by following the forward transition probability $P_F(s' | s) \propto F_\phi(s \rightarrow s')$ (Bengio et al., 2021a). It is worth noting that there exist other conditions equivalent to (3) that also yield similar guarantees for sampling proportionally to the reward function (Bengio et al., 2021b; Malkin et al., 2022; Madan et al., 2022). In particular, Deleu et al. (2022) used an alternative condition introduced by Bengio et al. (2021b) and inspired by the detailed-balance equations in the literature on Markov chains (see Section 3.3). In order to train the GFlowNet, it is possible to turn the target conditions such as the one in (3) into a corresponding loss function such that minimizing the loss makes the conditions satisfied, e.g.,

$$\mathcal{L}(\phi) = \mathbb{E}_\pi \left[\left(\log \frac{\sum_{s \in \text{Pa}(s')} F_\phi(s \rightarrow s')}{\sum_{s'' \in \text{Ch}(s')} F_\phi(s' \rightarrow s'') + R(s')} \right)^2 \right], \quad (4)$$

where π is some (full-support) distribution over the states of the GFlowNet.

3.3. GFlowNets for causal structure learning

Deleu et al. (2022) introduced a Bayesian structure learning algorithm based on GFlowNets, called *DAG-GFlowNet*, in order to approximate the (marginal) posterior over causal graphs $P(G | \mathcal{D})$. In this framework, a DAG is constructed by sequentially adding one edge at a time to the graph, starting from the fully disconnected graph over K nodes, with a special action to indicate when the generation ends and the current graph is a sample from the posterior approximation. A transition $G \rightarrow G'$ here then corresponds to adding one edge to G in order to obtain G' . Recall that a GFlowNet models a distribution proportional to the reward; therefore, DAG-GFlowNet uses $R(G) = P(\mathcal{D} | G)P(G)$ as the reward function in order to approximate the posterior distribution $P(G | \mathcal{D}) \propto R(G)$ once the GFlowNet is trained.

In order to train the GFlowNet, Deleu et al. (2022) used an alternative characterization of a flow network, different from the flow-matching conditions in (3). Instead of parametrizing the flows that once normalized yield the forward transition probability, they directly parametrized the forward transition probability $P_\phi(G' | G)$ with a neural network. Since all the states are valid samples from $P(G | \mathcal{D})$ (i.e., valid DAGs), they showed that for any transition $G \rightarrow G'$ in the GFlowNet, the detailed balance conditions (Bengio et al., 2021b) can be written as

$$R(G')P_B(G | G')P_\phi(s_f | G) = R(G)P_\phi(G' | G)P_\phi(s_f | G'), \quad (5)$$

where $P_B(G | G')$ is a fixed distribution over the parents of G' in the GFlowNet, and $P_\phi(s_f | G)$ is the probability of selecting the terminating action to return G and a sample from the posterior approximation. Similar to Section 3.2, one can show that if the conditions in (5) are satisfied for every transition $G \rightarrow G'$, then the GFlowNet also induces a distribution over objects proportional to the reward; in other words here, DAG-GFlowNet models the posterior distribution $P(G | \mathcal{D})$. Moreover, we can also turn those conditions into a loss function to train the parameters ϕ of the neural network, similar to the loss function in (4).

4. Variational Bayes-DAG-GFlowNet

One of the main limitations of DAG-GFlowNet (Deleu et al., 2022) is that it only approximates the marginal posterior distribution over graphs $P(G \mid \mathcal{D})$, and requires explicit marginalization over the mechanism parameters θ to compute the marginal likelihood $P(\mathcal{D} \mid G)$. In turn, this places strong assumptions on the causal mechanisms f between parents and child, such as linear-Gaussian relations, in order to make the computation of $P(\mathcal{D} \mid G)$ tractable.

In this work, we extend DAG-GFlowNet to model the posterior distribution $P(G, \theta \mid \mathcal{D})$ not only over the causal graphs G , but also on the parameters of the mechanisms θ .

To approximate the posterior distribution $P(G, \theta \mid \mathcal{D})$, we use Variational Bayes in conjunction with the GFlowNet. We model this posterior distribution using the following decomposition:

$$P(G, \theta \mid \mathcal{D}) \approx q_\phi(G)q_\lambda(\theta \mid G) = q_\phi(G) \prod_{k=1}^K q_\lambda(\theta_k \mid G), \quad (6)$$

where ϕ are the variational parameters of the distribution over graphs, λ are the parameters of the distribution over mechanism parameters, and θ_k are the parameters of the mechanism corresponding to the variable X_k . Using this factorization, it is possible to use Variational Bayes to alternatively update the distribution over graphs $q_\phi(G)$, and the distribution over parameters $q_\lambda(\theta \mid G)$. We can write the Evidence Lower-Bound (ELBO) for this model as $\log P(\mathcal{D}) \geq \text{ELBO}(\phi, \lambda)$, where

$$\begin{aligned} \text{ELBO}(\phi, \lambda) = \mathbb{E}_{G \sim q_\phi} [\mathbb{E}_{\theta \sim q_\lambda} [\log P(\mathcal{D} \mid \theta, G)] - \text{KL}(q_\lambda(\theta \mid G) \parallel P(\theta \mid G))] \\ - \text{KL}(q_\phi(G) \parallel P(G)). \quad (7) \end{aligned}$$

The derivation of the ELBO is available in [Appendix A.1](#). Variational Bayes corresponds to coordinate ascent on $\text{ELBO}(\phi, \lambda)$, alternatively maximizing it wrt. the parameters ϕ of the distribution over graphs, and wrt. the parameters λ of the distribution over mechanism parameters. Inspired by (Deleu et al., 2022), we use a GFlowNet in order to model the distribution $q_\phi(G)$ (where ϕ are the parameters of the GFlowNet). We call our method *Variational Bayes-DAG-GFlowNet* (VBG). The pseudo-code is available in [Algorithm 1](#).

4.1. Modelling the distribution over graphs with a GFlowNet

We show in [Appendix A.2](#) that maximizing the ELBO wrt. the parameters ϕ is equivalent to finding a distribution $q_{\phi^*}(G)$ such that, for any DAG G

$$\log q_{\phi^*}(G) = \mathbb{E}_{\theta \sim q_\lambda} [\log P(\mathcal{D} \mid \theta, G)] - \text{KL}(q_\lambda(\theta \mid G) \parallel P(\theta \mid G)) + \log P(G) + \text{const}, \quad (8)$$

where const is a constant term independent of G . Equivalently, we can see that the optimal distribution $q_{\phi^*}(G)$ is defined up to a normalizing constant: this is precisely a setting where GFlowNets can be applied. Unlike in [Section 3.3](#) though, where the reward was given by $R(G) = P(\mathcal{D} \mid G)P(G)$, here we can train the parameters ϕ of a GFlowNet with the reward function $\tilde{R}(G)$ defined as

$$\log \tilde{R}(G) = \mathbb{E}_{\theta \sim q_\lambda} [\log P(\mathcal{D} \mid \theta, G)] - \text{KL}(q_\lambda(\theta \mid G) \parallel P(\theta \mid G)) + \log P(G) \quad (9)$$

in order to find $q_{\phi^*}(G)$ that maximizes (7). In (9), the distribution $q_\lambda(\theta \mid G)$ corresponds to the current iterate of the distribution over mechanism parameters, found by maximizing the ELBO wrt.

λ at the previous iteration of coordinate ascent. Note that we can recover the same reward function as in DAG-GFlowNet by setting $q_\lambda(\theta | G) \equiv P(\theta | G)$. To find ϕ^* , we can then minimize the following loss functions, based on the conditions in (5)

$$\mathcal{L}(\phi) = \mathbb{E}_\pi \left[\left(\log \frac{\tilde{R}(G')P_B(G | G')P_\phi(s_f | G)}{\tilde{R}(G)P_\phi(G' | G)P_\phi(s_f | G')} \right)^2 \right], \quad (10)$$

where π is a (full-support) distribution over transitions $G \rightarrow G'$. Furthermore, similar to [Deleu et al. \(2022\)](#), we can efficiently compute the difference in log-rewards, the delta score, $\log \tilde{R}(G') - \log \tilde{R}(G)$, necessary for the loss function in (10):

$$\begin{aligned} \log \tilde{R}(G') - \log \tilde{R}(G) &= \mathbb{E}_{q_\lambda(\theta_j | G')} [\log P(X_j | \theta_j, G')] - \mathbb{E}_{q_\lambda(\theta_j | G)} [\log P(X_j | \theta_j, G)] \quad (11) \\ &\quad - \text{KL}(q_\lambda(\theta_j | G') \| P(\theta_j | G')) + \text{KL}(q_\lambda(\theta_j | G) \| P(\theta_j | G)) + \log P(G') - \log P(G) \end{aligned}$$

where $G \rightarrow G'$ corresponds to adding an edge $X_i \rightarrow X_j$ to G , in order to obtain G' . The proof of (11) is given in [Appendix A.3](#). Although applied in a different context, our work relates to the EB-GFN algorithm ([Zhang et al., 2022](#)) where an iterative procedure is used to update both a GFlowNet and the reward function (here, depending on q_λ), instead of having a fixed reward function. In practice we found that it was difficult to train the GFlowNet without it collapsing to a single graph using the above loss function (10), however if we introduce a hyper-parameter T which is inserted outside the log, we found that the GFlowNet is able to model the full posterior as seen in (12). This is not theoretically justified, and would correspond to something akin to learning the posterior to the power of the temperature parameter, however this alternative loss was used for all the experimental results. We found that setting the temperature to 0.5 works well all data generation schemes that were tested.

$$\mathcal{L}(\phi) = \mathbb{E}_\pi \left[\left(T \log \frac{\tilde{R}(G')P_B(G | G')P_\phi(s_f | G)}{\tilde{R}(G)P_\phi(G' | G)P_\phi(s_f | G')} \right)^2 \right], \quad (12)$$

4.2. Updating the distribution over mechanism parameters

Given the distribution over graphs $q_\phi(G)$, we want to find the parameters λ^* that maximize (7). To do so, a general recipe would be to apply gradient ascent over λ in $\text{ELBO}(\phi, \lambda)$, either for a few steps or until convergence ([Hoffman et al., 2013](#)). In some other cases though, we can obtain a closed form of the optimal distribution $q_{\lambda^*}(\theta | G)$, such as in linear-Gaussian models.

We present an example of the closed form update for a linear-Gaussian model here for completeness. In the case of a linear-Gaussian model, we can parametrize the mechanism parameters as a $K \times K$ matrix of edges weights, where θ_{ij} represents the strength of the connection between a parent X_i and a child variable X_j ; using this convention, θ_k in (6) corresponds to the k th column of this matrix of edge weights. We place a Gaussian prior $\theta_k \sim \mathcal{N}(\mu_0, \sigma_0^2 I_K)$ over the edge weights. The parameters λ of the distribution over mechanism parameters correspond to a collection of $\{(\mu_k, \Sigma_k)\}_{k=1}^K$, where for a given causal graph G

$$q_\lambda(\theta_k | G) = \mathcal{N}(D_k \mu_k, D_k \Sigma_k D_k) \quad \text{with} \quad D_k = \text{diag}(\{\mathbb{1}(X_i \in \text{Pa}_G(X_k))\}_{i=1}^K). \quad (13)$$

Algorithm 1: Finding the posterior distribution of DAGs and linear parameters

Data: A dataset \mathcal{D} .

Result: A distribution over graphs $q_\phi(G)$ & a distribution $q_\lambda(\theta | G)$ over mechanism parameters.

while *number of iterations* < *max iterations* **do**

while *delta loss of GFlowNet* > *min delta loss* **do**

 | Update the GFlowNet using $\tilde{R}(G)$ according to (9)

end

 Sample graphs from q_ϕ , modelled with the GFlowNet

 Calculate closed form update of μ & Σ according to (15) & (14), using sample graphs

end

In other words, the edge weights θ_k are parametrized by a Gaussian distribution and are then masked based on the parents of X_k in G . Note that the diagonal matrix D_k depends on the graph G , and therefore the covariance matrix $D_k \Sigma_k D_k$ is only positive semi-definite. We show in [Appendix A.4](#) that given the distribution over graphs $q_\phi(G)$, the optimal parameters μ_k and Σ_k maximizing (7) have the following closed-form:

$$\Sigma_k^{-1} = \frac{1}{\sigma_0^2} I_K + \frac{1}{\sigma^2} \mathbb{E}_{G \sim q_\phi} [D_k X^T X D_k] \quad (14)$$

$$\mu_k = \Sigma_k \left[\frac{1}{\sigma_0^2} \mu_0 + \frac{1}{\sigma^2} X_k^T X \mathbb{E}_{G \sim q_\phi} [D_k] \right] \quad (15)$$

where X is the $N \times K$ design matrix of the data set \mathcal{D} , X_k is its k th column, and σ^2 is the variance of the likelihood of the data, which is a hyper-parameter we set to 1. Note that while the true posterior distribution $P(\theta_k | G, \mathcal{D})$ is also a Normal distribution under a linear-Gaussian model, we are still making a variational assumption here by having common parameters μ_k and Σ_k across graphs, and samples θ_k are then masked according to D_k .

4.3. Assumptions

A number of assumptions are made in order to model the posterior over DAGs and mechanism parameters. The first is that we assume faithfulness; conditional independences observed in the data distribution correspond to conditional independences reflected in the graph, rather than from specific assignments of mechanisms that may give rise to conditional independence relations which are not present in the true graph. The second, we assume causal sufficiency; there are no unobserved confounders in the data. These two assumptions are common assumptions made about the data and the model in causal structure learning. Thirdly, we assume that it is sufficient to model the mechanisms as multivariate Gaussians where the relation of parent-child nodes are linear. Though this assumption is not essential to the algorithm, it served well as the first proof of concept for this method. And finally, we make an assumption when modeling the approximate posterior over mechanism parameters $q_\lambda(\theta | G)$. The approximate posterior over mechanism parameters is in practice learned jointly over all graphs, then the inferred θ 's are masked using specific graphs sampled from the distribution $q_\phi(G)$ to find the corresponding distribution for individual graphs $q_\lambda(\theta | G)$, as

shown in (13). Without this approximation, it would be necessary to learn an approximate posterior over mechanism parameters for each graph G samples from the posterior.

5. Experiments

We compare our method to other causal structure learning algorithms that are able to learn a distribution over the mechanisms and graphs using data sampled from synthetic graphs where the ground truth is known. We examine the performance of methods by comparing the learned graphs to the ground truth graph, as well as the estimated posterior to the true posterior of graphs. Comparison of posteriors was only done for graphs with 5 nodes, where it is possible to enumerate all possible DAGs. We find that our method, VBG does comparably well to other methods across metrics.

5.1. Data generation

Experiments were conducted on $K = 20$ node graphs with 40 total edges in expectation and $K = 5$ node graphs with 5 total edges in expectation. Graphs were generated according to the Erdos-Renyi random graph model (Erdős and Rényi, 1959). Results for each method were computed from 20 seeds with different graphs and data. The mechanisms between parent and child nodes were linear Gaussians, with the edge weights sampled uniformly in $\{-2, -0.5\} \cup \{0.5, 2.0\}$ as done in Cundy et al. (2021). Given the ground truth graph, data was sampled from the graph using ancestral sampling with a variance of $\sigma^2 = 0.1$. We used $N = 500$ samples of data for each experiment.

5.2. Baselines

We compared VBG (this paper) to other methods that infer both the graph and the mechanisms. First some recent gradient based posterior inference methods, DiBS (Lorch et al., 2021) and BCD Nets (Cundy et al., 2021). In addition, we also compared against two MCMC graph finding methods Metropolis-Hastings MCMC and Metropolis-within-Gibbs with adjustments to find the linear Gaussian parameters as introduced in (Lorch et al., 2021), these are referred to as Gibbs and MH in the figures and tables. Finally, we compared to GES (Chickering, 2003) and the PC algorithm (Spirtes et al., 2000) using DAG bootstrap (Friedman et al., 1999) to obtain a distribution over graphs and parameters.

For each metric, when calculating the expected value over graphs or parameters, 1000 samples each from the posterior over parameters and graphs are used. For DiBS, approximately 1000 samples of the posterior were used, since the algorithm does not guarantee cyclic graphs, they were filtered out before calculating the metrics. For all the methods except BCD-nets, the variance of the likelihood of the model was set to 0.1, this matches the variance that was used to generate the data. For BCD-nets the variance that is learned from the model was used to calculate the negative log-likelihood and the comparison to the true posterior. A uniform prior was used for all Bayesian methods (Bootstrap GES and PC are not Bayesian methods as there is no prior encoded), except for 20 node experiments with DiBS where an Erdos-Renyi prior was used. This is because DiBS requires sampling from the prior distribution of graphs for inference, and this is not possible with a uniform prior with more than 5 nodes. This could have resulted in a slight advantage for DiBS compared to other methods as the prior matches the true distribution of graphs.

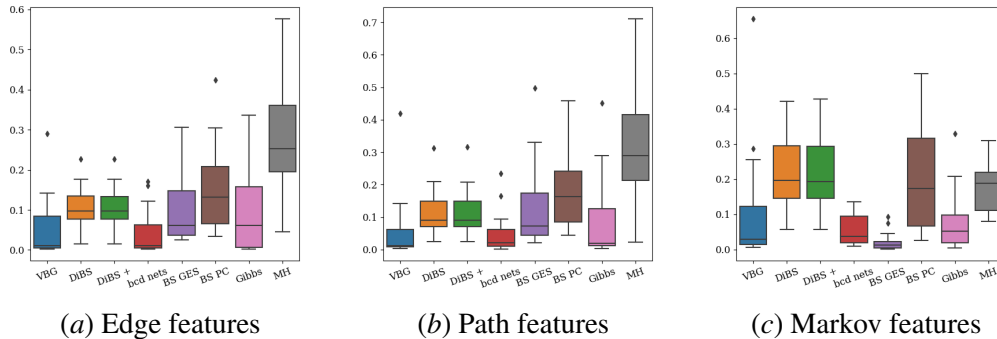


Figure 1: RMSE between Edge, path and Markov features of the true posterior and the estimated posterior for 5 node graphs. 1000 samples were taken from the true posterior and compared against the true posterior. Results were calculated across 20 different graphs. For all three metrics, the lower the better.

5.3. Comparing the approximate posterior to the ground truth posterior

We look at different features of the estimated posterior samples and compare them to the true posterior for 5 node graphs. These are done by looking at three properties; edge, path and Markov features. We calculate edge features by looking at each pair of nodes and counting the proportion of graphs where this edge exists in samples from the posterior estimate, then compare this to the proportion of graphs where the edge appears in the true posterior. (Friedman and Koller, 2000). With path features, we look at each pair of nodes and calculate the proportion of graphs from the estimated posterior where a directed path exists from one node to another, and compares this with the proportion of graphs where this path exists in the true posterior. Similarly with Markov features, for each pair of nodes, the proportion of graphs where two nodes are in the same Markov blanket in graphs from the estimated posterior is compared in samples of the true posterior. In summary, edge features reflect the distribution of graphs at the most fine-grained scale, compared to the other two metrics. Path features tells us about a longer range relationship between nodes in the graph. Markov features tell us about conditional relationships between nodes the in the graph, arguably the most important feature. Note that these metrics only depend on the posterior over graphs and not parameters. All priors for benchmark methods are uniform priors, to match the uniform prior which was used in VBG. VBG does consistently well across all three metrics compared to baselines suggesting that VBG well captures the posterior. Figure 1.

5.4. Comparing the ground truth graph with samples from the learned the posterior

We look at metrics often quoted for pairwise comparison of graph structures. Expected structural hamming distance (\mathbb{E} -SHD) represents the number of edge insertions deletions or flips in order to change the estimated graph to the ground truth graph, the lower the better. The area under the ROC graph (AUROC; Husmeier, 2003) informs of the number of true positive edges and false positive edges predicted from the algorithm, the higher the better. These two metrics are more suited to maximum-likelihood estimates of graphs since they only compare against a single ground truth graph, but we include them nonetheless since they are also reported by other similar works. To

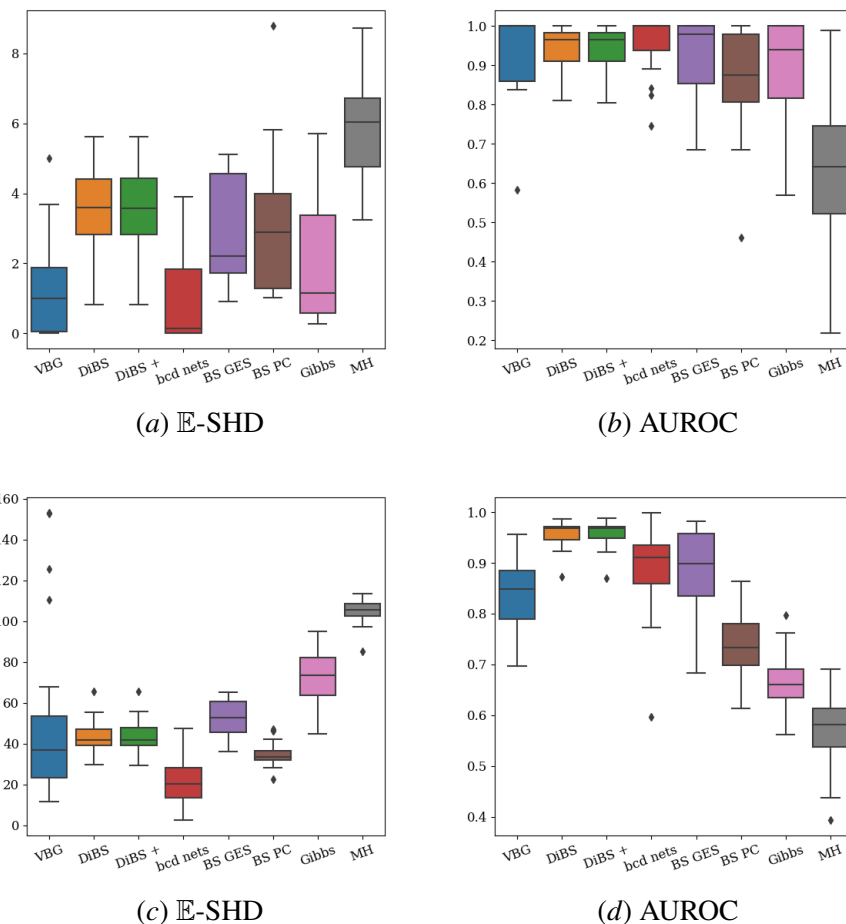


Figure 2: Modelling the posterior distribution over graphs and linear parameters and comparing to the ground truth graph and mechanism parameters θ . The top row, (a), (b), show results for 5 nodes and 5 edges in expectation. The bottom row (c), (d), show results for 20 nodes and 40 edges in expectation. Means and confidence intervals for each metric were calculated from data from 20 seeds, inferring 20 different graphs.

to assess the quality of the estimates of the mechanism parameters, we look at mean squared error of the mechanism parameters compared to the mechanism parameters of the true graph, as well as negative log likelihood of unseen data given the learned posterior over graphs. As a result of the large variance of these results across methods, they are presented as tables for 5 nodes in [Table 1](#) and [Table 2](#) and for 20 nodes in [Table 3](#) and [Table 4](#). Mean squared error is lowest for BCD-nets for both 5 and 20 nodes, and BS-GES performs the best for both number of nodes in-terms of negative log likelihood. In summary, VBG is competitive against baseline methods across these metrics but does not outperform baseline methods. We attribute the bias of the estimates of the graphs and parameters for VBG to the approximation made to estimate the posterior over parameters. The approximate posterior over parameters is learned jointly for all graphs in the posterior, and should in

practice, be learned for each graph. Masking of posterior distribution of parameters using adjacency matrices of graphs is used to distinguish between the approximate posterior between two neighboring graphs in the GFlowNet to calculate the delta score (11). This simplifies the computation of the mechanism parameters, removing the need to store the distinct mechanism parameters that could be learned for each graph sampled from the posterior. This approach could have led to misguided values of the updates of the mechanism parameters. At the expense of memory and computational complexity, these assumptions could be removed, which may lead to better estimates of the graphs and mechanism parameters for VBG.

quantiles	VBG	DiBS	DiBS +	BCD-nets	BS GES	BS PC	Gibbs	MH
0.50	0.01	0.86	0.86	0.00	0.06	0.12	3.20	0.34
0.25	0.00	0.75	0.74	0.00	0.03	0.04	2.36	0.24
0.75	0.11	1.00	1.00	0.05	0.16	0.26	3.88	0.46

Table 1: MSE of mechanism parameters for 5 nodes.

quantiles	VBG	DiBS	DiBS +	BCD-nets	BS GES	BS PC	Gibbs	MH
0.50	140.95	146.61	146.70	143.27	139.62	154.25	144.64	597.15
0.25	133.31	136.56	136.56	134.45	132.59	138.52	134.86	385.56
0.75	153.91	155.26	154.34	149.05	144.93	210.75	197.62	972.23

Table 2: Negative log likelihood of unseen data for 5 nodes.

quantiles	VBG	DiBS	DiBS +	BCD-nets	BS GES	BS PC	Gibbs	MH
0.50	0.09	2.25	2.23	0.05	0.09	0.12	0.63	0.16
0.25	0.04	2.03	2.06	0.04	0.06	0.11	0.59	0.15
0.75	0.13	2.53	2.53	0.07	0.12	0.14	0.68	0.18

Table 3: MSE of mechanism parameters for 20 nodes

quantiles	VBG	DiBS	DiBS +	BCD-nets	BS GES	BS PC	Gibbs	MH
0.50	1030.16	1042.96	1056.19	1004.30	724.38	3696.77	2384.62	6065.18
0.25	807.81	973.65	978.03	800.68	629.77	3039.66	1834.11	4414.87
0.75	1407.86	1226.75	1340.41	1070.78	958.34	5754.65	3414.39	9407.76

Table 4: Negative log likelihood of unseen data for 20 nodes.

6. Conclusion

We propose a novel method to model the posterior distribution over DAGs and linear Gaussian correlation coefficients between random variables using GFlowNets and Variational Bayes we call Variational Bayes DAG-GFlowNet (VBG). We found that the approximate posterior inferred using VBG was able to model the true posterior when inspecting 5-node graphs but did not outperform

other baseline methods across metrics comparing the true posterior to the estimated posterior, or metrics related to comparing the true graph to the estimated graph.

Even though VBG did not outperform existing methods, We believe that VBG offers something new to the toolbox for Bayesian causal structure learning in several ways. First, since VBG returns DAGs at every step of the training iteration, it lends itself well to using Variational Bayes to learn aspects of the causal model and the graph in this alternating step-wise procedure. Other existing Bayesian causal structure learning algorithms (Lorch et al., 2021; Annadani et al., 2021) rely on a soft acyclicity prior (Zheng et al., 2018) that does not guarantee sampling of DAGs, and often return a large proportion of cyclic graphs at the start of training. This may make these methods not amenable to iterative modelling and updating of graphs and other aspects of the causal model, as was done in VBG. In addition, the VBG setup could be extended to not just learning aspects of the causal model, but also to more fine-grained aspects of causal modeling such as inferring latent variables, or conversely for higher-level objects which are functions of the causal model as was suggested in Toth et al. (2022). Once VBG is trained, there is no upper limit on the number of samples that can be sampled from the posterior. This is in contrast to DiBS (Lorch et al., 2021), where the number of samples of the posterior must be pre-specified before training the model. In this paper, a linear Gaussian mechanism was assumed however the Variational Bayes approach does not rely on this assumption, and in theory, a non-linear function could parametrize the mechanism. This would yield something different from BCD Nets (Cundy et al., 2021), which relies on a linear Gaussian mechanism.

In future research, we would like to extend this work to non-linear functions by parametrizing the mechanisms using a single amortized neural network. Another avenue for future research is the application of VBG for active intervention targeting for causal structure learning (Scherrer et al., 2021; Agrawal et al., 2019; Tigas et al., 2022; Toth et al., 2022). Now that GFlowNets can be used for Bayesian causal structure learning of mechanisms and graphs, active intervention strategies can be used in conjunction with the method to inform what are the most informative interventions to take to learn about the causal model.

Acknowledgements

We would like to thank Dhanya Sridhar for the interesting discussions related to the project and causality, and Maxime Gasse for his feedback on the paper. This research was partially supported by the Canada CIFAR AI Chair Program. Yoshua Bengio is a CIFAR Senior Fellow.

References

- Raj Agrawal, Chandler Squires, Karren Yang, Karthik Shanmugam, and Caroline Uhler. Abcd-strategy: Budgeted experimental design for targeted causal structure discovery, 2019. URL <https://arxiv.org/abs/1902.10347>.
- Yashas Annadani, Jonas Rothfuss, Alexandre Lacoste, Nino Scherrer, Anirudh Goyal, Yoshua Bengio, and Stefan Bauer. Variational causal networks: Approximate bayesian inference over causal structures. *CoRR*, abs/2106.07635, 2021. URL <https://arxiv.org/abs/2106.07635>.

- Titus O. Awokuse. Export-led growth and the Japanese economy: evidence from VAR and directed acyclic graphs. *Applied Economics Letters*, 12(14):849–858, 2005. doi: 10.1080/13504850500358801. URL <https://doi.org/10.1080/13504850500358801>.
- Anastasiya Belyaeva, Chandler Squires, and Caroline Uhler. DCI: learning causal differences between gene regulatory networks. *Bioinformatics*, 37(18):3067–3069, 03 2021. ISSN 1367-4803. doi: 10.1093/bioinformatics/btab167. URL <https://doi.org/10.1093/bioinformatics/btab167>.
- Emmanuel Bengio, Moksh Jain, Maksym Korablyov, Doina Precup, and Yoshua Bengio. Flow Network based Generative Models for Non-Iterative Diverse Candidate Generation. *Neural Information Processing Systems*, 2021a.
- Yoshua Bengio, Tristan Deleu, Edward J. Hu, Salem Lahlou, Mo Tiwari, and Emmanuel Bengio. Gflownet foundations, 2021b. URL <https://arxiv.org/abs/2111.09266>.
- Philippe Brouillard, Sébastien Lachapelle, Alexandre Lacoste, Simon Lacoste-Julien, and Alexandre Drouin. Differentiable causal discovery from interventional data. *ArXiv*, abs/2007.01754, 2020.
- David Maxwell Chickering. Optimal structure identification with greedy search. *J. Mach. Learn. Res.*, 3(null):507–554, mar 2003. ISSN 1532-4435. doi: 10.1162/153244303321897717. URL <https://doi.org/10.1162/153244303321897717>.
- David Maxwell Chickering, Dan Geiger, and David Heckerman. Learning Bayesian networks: Search methods and experimental results. In Doug Fisher and Hans-Joachim Lenz, editors, *Pre-proceedings of the Fifth International Workshop on Artificial Intelligence and Statistics*, volume R0 of *Proceedings of Machine Learning Research*, pages 112–128. PMLR, 04–07 Jan 1995. URL <https://proceedings.mlr.press/r0/chickering95a.html>. Reissued by PMLR on 01 May 2022.
- Shrabanti Chowdhury, Ru Wang, Qing Yu, Catherine J. Huntoon, Larry M. Karnitz, Scott H. Kaufmann, Steven P. Gygi, Michael J. Birrer, Amanda G. Paulovich, Jie Peng, and Pei Wang. Dagbagn: Learning directed acyclic graphs of mixed variables with an application to identify prognostic protein biomarkers in ovarian cancer. *bioRxiv*, 2020. doi: 10.1101/2020.10.26.349076. URL <https://www.biorxiv.org/content/early/2020/10/27/2020.10.26.349076>.
- Chris Cundy, Aditya Grover, and Stefano Ermon. Bcd nets: Scalable variational approaches for Bayesian causal discovery. In *NeurIPS*, 2021.
- Tristan Deleu, António Góis, Chris Emezue, Mansi Rankawat, Simon Lacoste-Julien, Stefan Bauer, and Yoshua Bengio. Bayesian Structure Learning with Generative Flow Networks. *Conference on Uncertainty in Artificial Intelligence*, 2022.
- P Erdős and A Rényi. On random graphs i. *Publicationes Mathematicae Debrecen*, 6:290–297, 1959.
- Nir Friedman and Daphne Koller. Being Bayesian about network structure. *ArXiv*, abs/1301.3856, 2000.

- Nir Friedman, Moisés Goldszmidt, and Abraham J. Wyner. Data analysis with bayesian networks: A bootstrap approach. *ArXiv*, abs/1301.6695, 1999.
- Dan Geiger and David Heckerman. Learning gaussian networks. *CoRR*, abs/1302.6808, 2013. URL <http://arxiv.org/abs/1302.6808>.
- Matthew D Hoffman, David M Blei, Chong Wang, and John Paisley. Stochastic variational inference. *Journal of Machine Learning Research*, 2013.
- Patrik Hoyer, Dominik Janzing, Joris M Mooij, Jonas Peters, and Bernhard Schölkopf. Nonlinear causal discovery with additive noise models. In D. Koller, D. Schuurmans, Y. Bengio, and L. Bottou, editors, *Advances in Neural Information Processing Systems*, volume 21. Curran Associates, Inc., 2008. URL <https://proceedings.neurips.cc/paper/2008/file/f7664060cc52bc6f3d620bcedc94a4b6-Paper.pdf>.
- Dirk Husmeier. Sensitivity and specificity of inferring genetic regulatory interactions from microarray experiments with dynamic Bayesian networks. *Bioinformatics*, 19(17):2271–2282, 11 2003. ISSN 1367-4803. doi: 10.1093/bioinformatics/btg313. URL <https://doi.org/10.1093/bioinformatics/btg313>.
- Nan Rosemary Ke, Olexa Bilaniuk, Anirudh Goyal, Stefan Bauer, H. Larochelle, Chris Pal, and Yoshua Bengio. Learning Neural Causal Models from Unknown Interventions. *ArXiv*, abs/1910.01075, 2019.
- Nan Rosemary Ke, Silvia Chiappa, Jane X. Wang, Jörg Bornschein, Théophane Weber, Anirudh Goyal, Matthew Botvinic, Michael Curtis Mozer, and Danilo Jimenez Rezende. Learning to Induce Causal Structure. *ArXiv*, abs/2204.04875, 2022.
- Sébastien Lachapelle, Philippe Brouillard, Tristan Deleu, and Simon Lacoste-Julien. Gradient-based neural DAG learning. *CoRR*, abs/1906.02226, 2019. URL <http://arxiv.org/abs/1906.02226>.
- Lars Lorch, Jonas Rothfuss, Bernhard Schölkopf, and Andreas Krause. Dibs: Differentiable bayesian structure learning. *CoRR*, abs/2105.11839, 2021. URL <https://arxiv.org/abs/2105.11839>.
- Kanika Madan, Jarrid Rector-Brooks, Maksym Korablyov, Emmanuel Bengio, Moksh Jain, Andrei Nica, Tom Bosc, Yoshua Bengio, and Nikolay Malkin. Learning GFlowNets from partial episodes for improved convergence and stability. *arXiv preprint*, 2022.
- David Madigan and Jeremy York. Bayesian graphical models for discrete data. *International Statistical Review*, 63:215–232, 1995.
- Nikolay Malkin, Moksh Jain, Emmanuel Bengio, Chen Sun, and Yoshua Bengio. Trajectory Balance: Improved Credit Assignment in GFlowNets. *Advances in Neural Information Processing Systems*, 2022.
- Judea Pearl. *Probabilistic Reasoning in Intelligent Systems: Networks of Plausible Inference*. Morgan Kaufmann Publishers Inc., San Francisco, CA, USA, 1988. ISBN 1558604790.

- Judea Pearl. *Causality: Models, Reasoning, and Inference*. Cambridge University Press, USA, 2000. ISBN 0521773628.
- Jonas Peters, Dominik Janzing, and Bernhard Schölkopf. *Elements of Causal Inference: Foundations and Learning Algorithms*. Adaptive Computation and Machine Learning. MIT Press, Cambridge, MA, 2017. ISBN 978-0-262-03731-0. URL <https://mitpress.mit.edu/books/elements-causal-inference>.
- Nino Scherrer, Olexa Bilaniuk, Yashas Annadani, Anirudh Goyal, Patrick Schwab, Bernhard Schölkopf, Michael C. Mozer, Yoshua Bengio, Stefan Bauer, and Nan Rosemary Ke. Learning neural causal models with active interventions, 2021. URL <https://arxiv.org/abs/2109.02429>.
- Shohei Shimizu, Patrik O. Hoyer, Aapo Hyvarinen, and Antti Kerminen. A linear non-gaussian acyclic model for causal discovery. *Journal of Machine Learning Research*, 7(72):2003–2030, 2006. URL <http://jmlr.org/papers/v7/shimizu06a.html>.
- P. Spirtes, C. Glymour, and R. Scheines. *Causation, Prediction, and Search*. MIT press, 2nd edition, 2000.
- Panagiotis Tigas, Yashas Annadani, Andrew Jesson, Bernhard Schölkopf, Yarin Gal, and Stefan Bauer. Interventions, where and how? experimental design for causal models at scale, 2022. URL <https://arxiv.org/abs/2203.02016>.
- Christian Toth, Lars Lorch, Christian Knoll, Andreas Krause, Franz Pernkopf, Robert Peharz, and Julius von Kügelgen. Active bayesian causal inference. *ArXiv*, abs/2206.02063, 2022.
- Ioannis Tsamardinos, Laura Brown, and Constantin Aliferis. The max-min hill-climbing bayesian network structure learning algorithm. *Machine Learning*, 65:31–78, 10 2006. doi: 10.1007/s10994-006-6889-7.
- Tom S. Verma and Judea Pearl. On the equivalence of causal models. *CoRR*, abs/1304.1108, 1990. URL <http://arxiv.org/abs/1304.1108>.
- Benjie Wang, Matthew R Wicker, and Marta Kwiatkowska. Tractable uncertainty for structure learning. In *International Conference on Machine Learning*, pages 23131–23150. PMLR, 2022.
- Dinghuai Zhang, Nikolay Malkin, Zhen Liu, Alexandra Volokhova, Aaron Courville, and Yoshua Bengio. Generative Flow Networks for Discrete Probabilistic Modeling. *International Conference on Machine Learning*, 2022.
- Xun Zheng, Bryon Aragam, Pradeep Ravikumar, and Eric P. Xing. Dags with no tears: Continuous optimization for structure learning, 2018. URL <https://arxiv.org/abs/1803.01422>.

Appendix A. Proofs

A.1. Evidence Lower-Bound

In this section, we will prove the Evidence Lower-Bound (ELBO) in (7), which we recall here:

$$\log P(\mathcal{D}) \geq \mathbb{E}_{G \sim q_\phi} \left[\mathbb{E}_{\theta \sim q_\lambda} [\log P(\mathcal{D} \mid \theta, G)] - \text{KL}(q_\lambda(\theta \mid G) \parallel P(\theta \mid G)) \right] - \text{KL}(q_\phi(G) \parallel P(G)).$$

We start by writing the joint model between the data, causal graphs, and mechanism parameters as

$$P(\mathcal{D}, \theta, G) = P(\mathcal{D} \mid \theta, G)P(\theta \mid G)P(G)$$

Similarly, recall the the variational model for the approximation of the joint distribution can be factorized as $q(\theta, G) = q_\phi(G)q_\lambda(\theta \mid G)$. Therefore, using Jensen's inequality, we have:

$$\begin{aligned} \log P(\mathcal{D}) &= \log \left(\sum_G \int P(\mathcal{D}, \theta, G) d\theta \right) \\ &= \log \left(\sum_G \left[\int \frac{P(\mathcal{D}, \theta, G)}{q_\phi(G)q_\lambda(\theta \mid G)} q_\lambda(\theta \mid G) d\theta \right] q_\phi(G) \right) \\ &\geq \sum_G \left[\int \log \frac{P(\mathcal{D}, \theta, G)}{q_\phi(G)q_\lambda(\theta \mid G)} q_\lambda(\theta \mid G) d\theta \right] q_\phi(G) \\ &= \sum_G \left[\int \log \frac{P(\mathcal{D} \mid \theta, G)P(\theta \mid G)P(G)}{q_\phi(G)q_\lambda(\theta \mid G)} q_\lambda(\theta \mid G) d\theta \right] q_\phi(G) \\ &= \sum_G \left[\int \log (P(\mathcal{D} \mid \theta, G)) q_\lambda(\theta \mid G) d\theta + \int \log \frac{P(\theta \mid G)}{q_\lambda(\theta \mid G)} q_\lambda(\theta \mid G) d\theta + \log \frac{P(G)}{q_\phi(G)} \right] q_\phi(G) \\ &= \sum_G \left[\mathbb{E}_{\theta \sim q_\lambda} [\log P(\mathcal{D} \mid \theta, G)] - \text{KL}(q_\lambda(\theta \mid G) \parallel P(\theta \mid G)) + \log \frac{P(G)}{q_\phi(G)} \right] q_\phi(G) \\ &= \mathbb{E}_{G \sim q_\phi} \left[\mathbb{E}_{\theta \sim q_\lambda} [\log P(\mathcal{D} \mid \theta, G)] - \text{KL}(q_\lambda(\theta \mid G) \parallel P(\theta \mid G)) \right] - \text{KL}(q_\phi(G) \parallel P(G)) \end{aligned}$$

A.2. Maximization of the ELBO wrt. the distribution over graphs

We want to show that the distribution q_{ϕ^*} that maximizes $\text{ELBO}(\phi, \lambda)$ in (7) wrt. the parameters ϕ of the distribution over graphs is given by

$$\log q_{\phi^*}(G) = \mathbb{E}_{\theta \sim q_\lambda} [\log P(\mathcal{D} \mid \theta, G)] - \text{KL}(q_\lambda(\theta \mid G) \parallel P(\theta \mid G)) + \log P(G) + \text{const},$$

where const is a constant term independent of the graph G . We know that there is a finite number of possible DAGs that one can create over K nodes, and we can denote them as $\{G_1, \dots, G_M\}$ (where M is the number of possible DAGs over K nodes, which is super-exponential in K). The maximization problem we want to solve can be written as the following constrained optimization problem:

$$\begin{aligned} &\max_{\{q_\phi(G_m)\}_{m=1}^M} \text{ELBO}(q_\phi, q_\lambda) \\ &\text{s.t.} \quad \sum_{m=1}^M q_\phi(G_m) = 1, \end{aligned}$$

where we made the dependence of the ELBO on q_ϕ and q_λ more explicit. To find the solutions of this constrained optimization problem, we can look for the critical points of the Lagrangian, defined as:

$$\begin{aligned} L(\{q_\phi(G_m)\}_{m=1}^M, \eta) &= \text{ELBO}(q_\phi, q_\lambda) + \eta \left(\sum_{m=1}^M q_\phi(G_m) - 1 \right) \\ &= \sum_{m=1}^M \left[\mathbb{E}_{\theta \sim q_\lambda} [\log P(\mathcal{D} \mid \theta, G_m)] - \text{KL}(q_\lambda(\theta \mid G_m) \parallel P(\theta \mid G_m)) + \right. \\ &\quad \left. \log \frac{P(G_m)}{q_\phi(G_m)} + \eta \right] q_\phi(G_m) - \eta \end{aligned}$$

Taking the derivative of the Lagrangian wrt. a particular $q_\phi(G_m)$, and equating it to 0, we get

$$\begin{aligned} \frac{\partial L}{\partial q_\phi(G_m)} &= \mathbb{E}_{\theta \sim q_\lambda} [\log P(\mathcal{D} \mid \theta, G_m)] - \text{KL}(q_\lambda(\theta \mid G_m) \parallel P(\theta \mid G_m)) \\ &\quad + \log P(G_m) - \log q_{\phi^*}(G_m) - 1 + \eta = 0 \end{aligned}$$

$$\Leftrightarrow \log q_{\phi^*}(G_m) = \mathbb{E}_{\theta \sim q_\lambda} [\log P(\mathcal{D} \mid \theta, G_m)] - \text{KL}(q_\lambda(\theta \mid G_m) \parallel P(\theta \mid G_m)) + \log P(G_m) + \text{const}$$

A.3. Derivation of the difference in log-rewards

Recall that the reward of the GFlowNet used in VBG is defined as

$$\log \tilde{R}(G) = \mathbb{E}_{\theta \sim q_\lambda} [\log P(\mathcal{D} \mid \theta, G)] - \text{KL}(q_\lambda(\theta \mid G) \parallel P(\theta \mid G)) + \log P(G).$$

Since the loss function in (10) only depends on the difference in log-reward $\log \tilde{R}(G') - \log \tilde{R}(G)$, we can show that this can be written as

$$\begin{aligned} \log \tilde{R}(G') - \log \tilde{R}(G) &= \mathbb{E}_{q_\lambda(\theta_j \mid G')} [\log P(X_j \mid \theta_j, G')] - \mathbb{E}_{q_\lambda(\theta_j \mid G)} [\log P(X_j \mid \theta_j, G)] \\ &\quad - \text{KL}(q_\lambda(\theta_j \mid G') \parallel P(\theta_j \mid G')) + \text{KL}(q_\lambda(\theta_j \mid G) \parallel P(\theta_j \mid G)) + \log P(G') - \log P(G), \end{aligned}$$

where $G \rightarrow G'$ is a transition in the GFlowNet after adding the edge $X_i \rightarrow X_j$ to G to obtain G' . This formula is a direct consequence of the decomposition of the observation model $P(\mathcal{D} \mid \theta, G)$ as given in (1), and the factorization of the prior over mechanism parameters $P(\theta \mid G)$ and the variational distribution $q_\lambda(\theta \mid G)$ (see (6)). When taking the difference in log-rewards, then only the term corresponding to the variable X_j changes, since this is the only mechanism that changes from G to G' after the addition of the edge $X_i \rightarrow X_j$. This result is akin to the delta-score commonly used in the structure learning literature.

A.4. Update of the variational distribution in linear-Gaussian case

For a specific variable X_k , recall that the prior for the linear-Gaussian model and the variational distribution q_λ can be written as

$$P(\theta_k \mid G) = \mathcal{N}(\mu_0, \sigma_0^2 I_K) \quad q_\lambda(\theta_k \mid G) = \mathcal{N}(D_k \mu_k, D_k \Sigma_k D_k),$$

where $D_k = \text{diag}(\{\mathbb{1}(X_i \in \text{Pa}_G(X_k))\}_{i=1}^K)$ is a diagonal matrix masking the variables X_i that are not parents of X_k in G . Moreover, we know that under a linear-Gaussian model, the observation model can be written as

$$X_k = \sum_{i=1}^K \mathbb{1}(X_i \in \text{Pa}_G(X_k)) \theta_{ik} X_i + \varepsilon_k \quad \text{where} \quad \varepsilon_k \sim \mathcal{N}(0, \sigma^2).$$

In other words, we can write X_k (as a vector of size N containing all the entries of variable X_k in \mathcal{D}) as a Normal vector of the form

$$P(X_k | \theta_k, \text{Pa}_G(X_k)) = \mathcal{N}(A_k \theta_k, \sigma^2 I_N) \quad \text{where} \quad A = X D_k,$$

and where X is the $N \times K$ design matrix for the dataset \mathcal{D} . Since we are masking the entries of X that are not parents of X_k in G directly, this is equivalent to not having to mask θ_k in the variational distribution q_λ . Therefore, we can assume that under this observation model, the variational distribution will be of the form $q_\lambda(\theta_k | G) = \mathcal{N}(\mu_k, \Sigma_k)$ (i.e., without masking the mean and covariance matrix). We want to find the parameters μ_k and Σ_k that maximize the ELBO in (7), we q_ϕ fixed. We can make the dependence of all the terms inside the expectation wrt. q_ϕ more explicit in μ_k and Σ_k , starting with the expected log-likelihood:

$$\begin{aligned} \mathbb{E}_{q_\lambda(\theta_k | G)} [\log P(X_k | \theta_k, \text{Pa}_G(X_k))] &= \mathbb{E}_{q_\lambda(\theta_k | G)} \left[-\frac{1}{2\sigma^2} \|X_k - A_k \theta_k\|^2 + \text{const} \right] \\ &= -\frac{1}{2\sigma^2} \mathbb{E}_{q_\lambda(\theta_k | G)} [\theta_k^T A_k^T A_k \theta_k - 2X_k^T A_k \theta_k] + \text{const} \\ &= -\frac{1}{2\sigma^2} \mathbb{E}_{q_\lambda(\theta_k | G)} [\text{Tr}(\theta_k^T A_k^T A_k \theta_k) - 2X_k^T A_k \theta_k] + \text{const} \\ &= -\frac{1}{2\sigma^2} \mathbb{E}_{q_\lambda(\theta_k | G)} [\text{Tr}(A_k^T A_k \theta_k \theta_k^T) - 2X_k^T A_k \theta_k] + \text{const} \\ &= -\frac{1}{2\sigma^2} [\text{Tr}(A_k^T A_k \mathbb{E}_{q_\lambda(\theta_k | G)} [\theta_k \theta_k^T]) - 2X_k^T A_k \mathbb{E}_{q_\lambda(\theta_k | G)} [\theta_k]] + \text{const} \\ &= -\frac{1}{2\sigma^2} [\text{Tr}(A_k^T A_k (\Sigma_k + \mu_k \mu_k^T)) - 2X_k^T A_k \mu_k] + \text{const} \\ &= -\frac{1}{2\sigma^2} [\text{Tr}(A_k^T A_k \Sigma_k) + \|A_k \mu_k\|^2 - 2X_k^T A_k \mu_k] + \text{const} \end{aligned}$$

Similarly, we can write the KL-divergence term more explicitly as a function of μ_k and Σ_k , using the explicit form of the KL-divergence between two multivariate Normal distributions:

$$\text{KL}(q_\lambda(\theta_k | G) \| P(\theta_k | G)) = \frac{1}{2} \left[\frac{1}{\sigma_0^2} \|\mu_0 - \mu_k\|^2 + \frac{1}{\sigma_0^2} \text{Tr}(\Sigma_k) - \log \det(\Sigma_k) \right] + \text{const}$$

Therefore the ELBO, seen as a function of only μ_k and Σ_k is

$$\begin{aligned} \text{ELBO}(\mu_k, \Sigma_k) &= -\frac{1}{2} \mathbb{E}_{G \sim q_\phi} \left[\frac{1}{\sigma^2} \text{Tr}(A_k^T A_k \Sigma_k) + \frac{1}{\sigma^2} \|A_k \mu_k\|^2 - \frac{1}{\sigma^2} 2X_k^T A_k \mu_k \right. \\ &\quad \left. + \frac{1}{\sigma_0^2} \|\mu_0 - \mu_k\|^2 + \frac{1}{\sigma_0^2} \text{Tr}(\Sigma_k) - \log \det(\Sigma_k) \right] + \text{const} \end{aligned}$$

Taking the derivative of the ELBO wrt. μ_k and Σ_k , we get

$$\begin{aligned} \frac{\partial \text{ELBO}}{\partial \Sigma_k} &= -\frac{1}{2} \mathbb{E}_{G \sim q_\phi} \left[\frac{1}{\sigma_0^2} I_K + \frac{1}{\sigma^2} A_k^T A_k - \Sigma_k^{-1} \right] = 0 \quad \Rightarrow \quad \Sigma_k^{-1} = \frac{1}{\sigma_0^2} I_K + \frac{1}{\sigma^2} \mathbb{E}_{G \sim q_\phi} [A_k^T A_k] \\ \frac{\partial \text{ELBO}}{\partial \mu_k} &= -\mathbb{E}_{G \sim q_\phi} \left[\frac{1}{\sigma^2} A_k^T A_k \mu_k - \frac{1}{\sigma^2} X_k^T A_k + \frac{1}{\sigma_0^2} (\mu_k - \mu_0) \right] = 0 \\ &\Leftrightarrow \mathbb{E}_{G \sim q_\phi} \left[\frac{1}{\sigma_0^2} I_K + \frac{1}{\sigma^2} A_k^T A_k \right] \mu_k = \frac{1}{\sigma_0^2} \mu_0 + \frac{1}{\sigma^2} X_k^T \mathbb{E}_{G \sim q_\phi} [A_k] \\ &\Rightarrow \mu_k = \Sigma_k \left[\frac{1}{\sigma_0^2} \mu_0 + \frac{1}{\sigma^2} X_k^T \mathbb{E}_{G \sim q_\phi} [A_k] \right] \end{aligned}$$

Therefore, the updates of the parameters μ_k and Σ_k that maximize the ELBO wrt. the parameters of the distribution q_λ are given by:

$$\begin{aligned} \mu_k &= \Sigma_k \left[\frac{1}{\sigma_0^2} \mu_0 + \frac{1}{\sigma^2} X_k^T X \mathbb{E}_{G \sim q_\phi} [D_k] \right] \\ \Sigma_k^{-1} &= \frac{1}{\sigma_0^2} I_K + \frac{1}{\sigma^2} \mathbb{E}_{G \sim q_\phi} [D_k X^T X D_k] \end{aligned}$$